

Electrooxidation and Electroreduction of Anthraquinone Chromophores at the Platinum Electrode

Anna Marzec^{1,*}, Ewa Chrzescijanska², Bolesław Szadkowski¹, Małgorzata Kuśmierk¹,
Marian Zaborski¹

¹ Lodz University of Technology, Institute of Polymer and Dye Technology, Faculty of Chemistry, 90-924 Lodz, ul Stefanowskiego 12/16, Poland

² Lodz University of Technology, Institute of General and Ecological Chemistry, Faculty of Chemistry, 90-924 Lodz, ul Zeromskiego 116, Poland

*E-mail: marzec.anna@hotmail.com

Received: 2 May 2019 / Accepted: 30 June 2019 / Published: 5 August 2019

This study investigates the electrochemical behavior of anthraquinone dyes in non-aqueous solution. Cyclic voltammetry and differential pulse voltammetry were used to estimate the electrochemical parameters of electrooxidation and electroreduction at the platinum electrode. The effects of different substituents on the electrochemical properties of solvent dyes were determined based on physico-chemical parameters such as the peak potential (E_{pa}), half-peak potential ($E_{pa/2}$) or half-wave potential ($E_{1/2}$). Theoretical methods were used to estimate the diffusion coefficients, solubility parameters and HOMO–LUMO gaps of the anthraquinone dyes. The structures and morphologies of the studied powders were also examined using scanning electron microscopy (SEM). Cyclic voltammograms showed multiple redox processes and revealed quasi-reversible behavior in all the studied dyes.

Keywords: electrochemistry; anthraquinone dyes; electrooxidation; electroreduction; Pt electrode

1. INTRODUCTION

Anthraquinone (Aq) compounds constitute a very extensive group of natural quinones which have a wide variety of chemical, biological and pharmacological uses [1, 2]. Hydroxyquinones are an especially prominent family of pharmaceutically active and biologically relevant chromospheres with important applications [3, 4]. Compounds recognized as quinones have a particular arrangement of C=O moieties in their molecules, i.e. structures containing two double bonds in a six-membered ring and two ketone carbonyl moieties, as presented in Figure 1 [1].

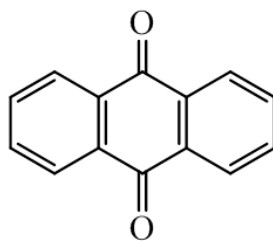


Figure 1. The chemical structure of 9,10-anthraquinone.

Anthraquinone colorants come in a wide variety of chemical structures. Almost all natural red dyes are anthraquinones, for instance the well-known alizarin dye (1,2-dihydroxyanthraquinone). Anthraquinone-based dyes are synthesized by the introduction of various substituents, such as $-\text{NH}_2$ or $-\text{OH}$ groups, into the anthraquinone structure, which is easily available via the oxidation of anthracene [5, 6]. After the introduction of electron-releasing groups into the anthraquinone nucleus, a bathochromic shift occurs. This shift depends primarily on such factors as the number of electron-releasing groups, their positions and their relative strengths. The strength of the electron-donor moieties increases in the following order: $\text{OH} < \text{NH}_2 < \text{NHR} < \text{HNPh}$ [7, 8]. Thus, they can be considered as classic donor-acceptor systems, containing auxochromes (electron-releasing moieties) which act as electron donors and carbonyl groups that act as acceptors. The electron-releasing groups exert their maximum bathochromic effect in the α -positions (1, 4, 5, 8) rather than the β -positions (2, 3, 6, 7). The typical substitution signals can be specified as follows: 1,4; 1,2,4; 1,4,5,8. Both hydroxyl and amino groups (primary and secondary) can be applied to optimize the properties of anthraquinone compounds. Moreover, α -substituents can give dyes higher values for molar extinction coefficients and, due to their strong intermolecular hydrogen bonding with $\text{C}=\text{O}$ groups, enhance their technical performance, especially light fastness.

Many different methods have been employed to examine various kinds of anthraquinone dyes. However, they are based mostly on spectrophotometric measurements, such as UV-Vis or fluorescence spectrophotometry. These kinds of techniques require expensive instruments and serious errors may arise when colored and/or muddy samples are evaluated. In contrast, electrochemical experiments do not require costly equipment and are suitable for colored and/or muddy samples. Currently, electrochemical methods for the measurement and characterization of dyes are being developed and improved [9-13]. There are many benefits to the application of electrochemical techniques, such as rapid analysis, high sensitivity and low cost [14]. Electroanalytical experiments, more specifically voltammetric methods, are very useful for studying the oxidation potential, the number of transferred electrons and the rate of the electrode reaction.

In recent years, the structure-property relationship of different dyes has drawn the interest of many scientists. Quantum chemical computation data have been employed to make quantitative predictions regarding the behavior of dyes, such as their chemical reactivity and physicochemical properties. The highest occupied molecular orbital (HOMO) and the lowest unoccupied molecular orbital (LUMO) energies may be useful when characterizing the activity of these compounds [15, 16]. It is known from the literature that the orbital determines the way in which a molecule interacts with

other species. The HOMO acts as an electron donor and is concentrated on the benzene ring. Therefore, it can be assumed that electrophilic attack will occur in this area. On the other hand, the LUMO acts as an electron acceptor and is mainly subjected to nucleophilic attack. Based on the highest occupied molecular orbital (HOMO)-lowest unoccupied molecular orbital (LUMO) energy separation (HOMO-LUMO gap – E_{gap}) the kinetic stability of the molecules can be estimated [17, 18].

Recently, a relatively new group of solvent dyes based on anthraquinone chromophores has attracted interest. These dyes have very good solubility in different non-polar media and exhibit extraordinary color strength, transparency as well as very high thermal and light stability. Another important advantage is their relatively low price. Due to the fact that these dyes have a large range of possible applications as colorants, it is particularly important to determine the susceptibility of their structures to oxidation and reduction. Research to date includes numerous studies on the electrochemical behavior of water-soluble anthraquinone (AQ) derivatives and alizarin derivatives [11, 12]. However, the electrochemical behavior of anthraquinone solvent dyes has not previously been described.

This work set out to perform a qualitative, systematic and comparative study of the electrooxidation and electroreduction of different organic chromophores (Table 1) using cyclic voltammetry (CV) and differential pulse voltammetry (DPV) with a platinum electrode. The parameters of the solvent dyes, the diffusion coefficients and quantum-chemical calculations were calculated theoretically. Scanning electron microscopy (SEM) was applied to investigate the structure and morphology of the studied dyes. The correlation between the structure of anthraquinone derivatives, the peak potential and theoretical parameters enabled qualitative classification of the compounds in terms of their oxidation and reduction capacities.

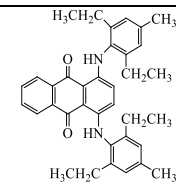
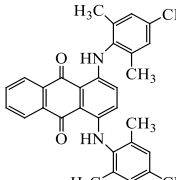
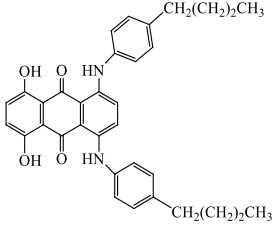
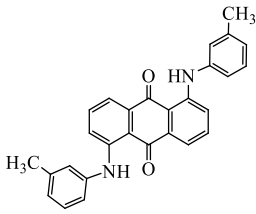
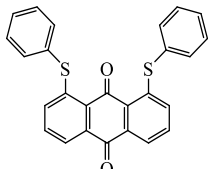
2. EXPERIMENTAL

2.1. Chemicals

Organic chromophores: 1,4-bis[2,6-diethyl-4-methylphenylamino]anthracene-9,10-dione (Keystone, USA), 1,4-bis[2,4,6-trimethylphenylamino]anthracene-9,10-dione (Keystone, USA), 1,4-bis[(4-n-butylphenyl)amino-5,8-dihydroxy]anthracene-9,10-dione (Keystone, USA), 1,5-bis[(3-methylphenyl)amino]anthracene-9,10-dione (Keystone, USA), 1,8-bis(phenylthio)anthracene-9,10-dione (Keystone, USA). The structures of the organic chromophores are shown in Table 1.

1-Methyl-2-pyrrolidinone ($\text{C}_5\text{H}_9\text{NO}$, pure p.a.) was supplied by Sigma-Aldrich and was used to prepare the amino acid solutions. Tetrabutylammonium perchlorate ($(\text{C}_4\text{H}_9)_4\text{NClO}_4$) was sourced from Fluka (Germany) and was used as a supporting electrolyte. The substrate was dissolved in 0.1 mol L^{-1} $(\text{C}_4\text{H}_9)_4\text{NClO}_4$ in 1-methyl-2-pyrrolidinone. The concentration of the dye was $1.0 \times 10^{-3} \text{ mol L}^{-1}$. All the reagents used were analytical grade.

Table 1. Chemical composition of the studied organic chromophores.

Nr	Color Index, name	Chemical structure	Symbol
1.	1,4-bis[2,6-diethyl-4-methylphenylamino]anthracene-9,10-dione		Dye 1
2.	1,4-bis[2,4,6-trimethylphenylamino]anthracene-9,10-dione		Dye 2
3.	1,4-bis[(4-n-butylphenyl)amino-5,8-dihydroxy]anthracene-9,10-dione		Dye 3
4.	1,5-bis[(3-methylphenyl)amino]anthracene-9,10-dione		Dye 4
5.	1,8-bis(phenylthio)anthracene-9,10-dione		Dye 5

2.2. Measurement methods

To assess the electrochemical oxidation mechanisms and kinetics of the compounds, cyclic voltammetry (CV) and differential pulse voltammetry (DPV) were used with an Autolab analytical unit (EcoChemie, Holland). A three-electrode system was used for the measurements. Platinum was used for the anode and auxiliary electrode. The electrode potential was measured against a ferricinium/ferrocene reference electrode (Fc^+/Fc), the standard potential of which was defined as zero, regardless of the solvent used. All of the solutions were degassed with argon prior to the measurements. During the measurements, an argon blanket was maintained over the solution. The effect of the scan rate on the electrooxidation of the solvent dyes and pigments in an anhydrous medium was assessed. Before the measurements, the solutions were purged with argon to remove any

dissolved oxygen. During the measurements, an argon blanket was kept over the solutions. All experiments were performed at room temperature.

Cyclic voltammetry (CV) involves varying the applied potential at the working electrode in both forward and reverse directions (at a certain scan rate) while monitoring the current. For example, an initial scan could be made in the positive direction to the switching potential. Then, the scan could be reversed and run in the negative direction. Depending on the analysis, one full cycle, a partial cycle or a series of cycles may be performed [19, 20]. Cyclic voltammograms (CV) were recorded for potentials of 0, 1.8 or 2.0 V with various scan rates (0.01 to 0.5 V s⁻¹).

Differential pulse voltammetry (DPV) is a scanning technique that uses a series of pulses. The potential of each pulse is fixed, of small amplitude (10 to 100 mV) and is superimposed on a slowly changing base potential. Current is measured at two points for each pulse, the first just before the application of the pulse and the second at the end of the pulse. The difference between the current measurements at these points for each pulse is determined and plotted against the base potential. Differential pulse voltammograms (DPV) were recorded for the same potential range with a modulation of amplitude 25 mV and pulse width of 50 ms (scan rate 0.01 V s⁻¹).

2.3. Kinetic parameters of dyes

The recorded voltammograms, under linear diffusion of the first step of electrooxidation, were used to determine the peak potential (E_{pa}), half-peak potential ($E_{pa/2}$) and half-wave potential ($E_{1/2}$). The voltammograms were also used to calculate the anodic transition coefficient (βn_{β}) and heterogeneous rate constant (k_{bh}) of the electrode process for the half-wave potential. The parameters were calculated according to the following equations [21]:

$$\beta n_{\beta} = \frac{1.857RT}{F(E_{pa} - E_{pa/2})} \quad (1)$$

$$E_{pa} = -1.14 \frac{RT}{\beta n_{\beta} F} - \frac{RT}{\beta n_{\beta} F} \ln \frac{k_{bh}^0}{D_{red}^{1/2}} + \frac{RT}{2\beta n_{\beta} F} \ln \beta n_{\beta} \nu \quad (2)$$

$$k_{bh} = k_{bh}^0 \exp\left(\frac{-\beta n_{\beta} FE}{RT}\right) \quad (3)$$

where: D_{red} is the diffusion coefficient of the reduced form, cm²s⁻¹; ν is the scan rate; V s⁻¹; F is the Faraday constant (96.487 C mol⁻¹); R is the universal gas constant (8.314 J K⁻¹mol⁻¹); T is Kelvin temperature.

The diffusion coefficients (D) of the solvent dyes and stabilizers were estimated using the method developed by Hayduk and Laudie [22]:

$$D = \frac{13.26 \times 10^{-5}}{\mu^{1.4} \nu_o^{0.589}} \quad (4)$$

where μ is the viscosity of the solvent (centipoises) and ν_o is the molar volume (cm³ g⁻¹ mole⁻¹).

The solubility parameters of the solvent dyes and stabilizers were predicted according to Kirevelen's method from the group contributions (δ_d – dispersion forces, δ_p – polar forces, δ_h – hydrogen-bonding forces, V – molar volume) using the following equations [23]:

$$\delta_d = \frac{\sum F_{di}}{V} ; \delta_p = \frac{\sqrt{\sum F_{pi}^2}}{V} ; \delta_h = \frac{\sqrt{\sum E_{hi}}}{V} \quad (5)$$

The differences in the solubility parameters ($\Delta\delta$) between the ethylene-norbornene copolymer and solvent dyes were calculated using Equation 6 [24].

$$\Delta\delta = \left[4(\delta_{d,P} - \delta_{d,D})^2 + (\delta_{p,P} - \delta_{p,D})^2 + (\delta_{h,P} - \delta_{h,D})^2 \right]^{\frac{1}{2}} \quad (6)$$

2.4. Quantum chemical calculations

Quantum chemical calculations were performed with HyperChem program packages using the AM1 method. The molecular structures of the dyes in gas phase were fully optimized using ab-initio quantum chemical calculations at the restricted Hartree–Fock (RHF) level of theory. The highest occupied molecular orbital (E_{HOMO}) and the lowest unoccupied molecular orbital (E_{LUMO}) were calculated.

2.5. Scanning Electron Microscopy (SEM)

The morphologies of the solvent dyes were estimated using SEM with a ZEISS SEM microscope. Prior to the measurements, the samples were coated with carbon.

3. RESULTS AND DISCUSSION

3.1. Electrochemical oxidation of anthraquinone dyes on Pt electrode

Electrochemical studies were performed using CV and DPV voltammetry to determine the activity of the tested dyes in oxidation and reduction reactions. Selected cyclic and differential pulse voltammograms showing the electrooxidation of the organic chromophores are presented in Figures 2 and 3. The half-wave potential ($E_{1/2}$) of the electrode reaction, as investigated by CV, corresponded to the peak potential (E_p) according to DPV.

As may be noticed, structures D1 and D2 oxidized in two electrode steps at potentials lower than those for electrolyte decomposition. Structures D3 and D4 oxidized in one step and the reactions were also irreversible. The exception was dye D5, which showed no peak oxidation potentials in the studied range. The voltammograms, recorded under linear diffusion, were used to determine the peak potential (E_{pa}), half-peak potential ($E_{pa/2}$) and half-wave potential ($E_{1/2}$). Half-wave potential ($E_{1/2}$) can provide information concerning the ability of organic chromophores to participate in redox reactions.

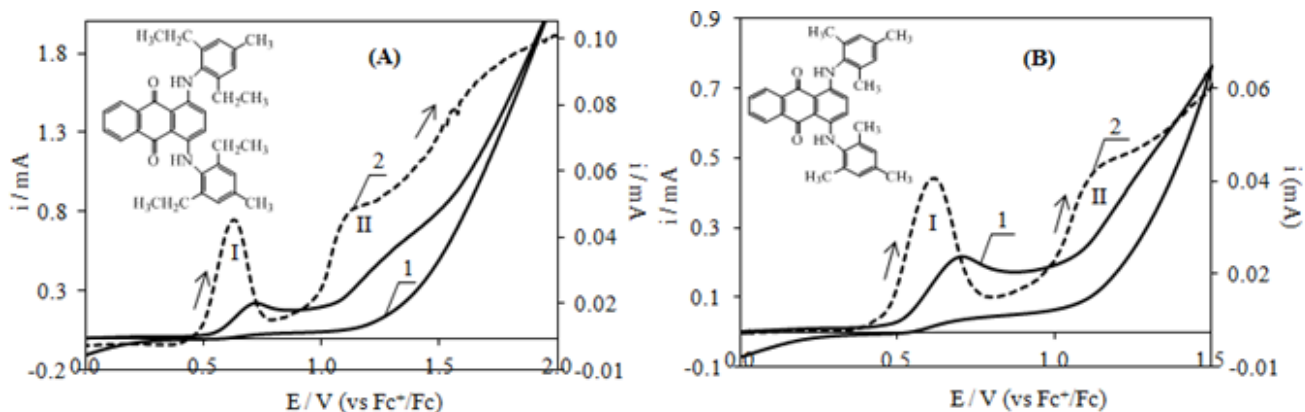


Figure 2. CV (curve 1) and DPV (curve 2) of (A) D1 and (B) D2 oxidation at Pt electrode; $c = 1.0 \times 10^{-3}$ M in 0.1 M $(C_4H_9)_4NClO_4$ in 1-methyl-2-pyrrolidinone; $v = 0.1$ V s^{-1} .

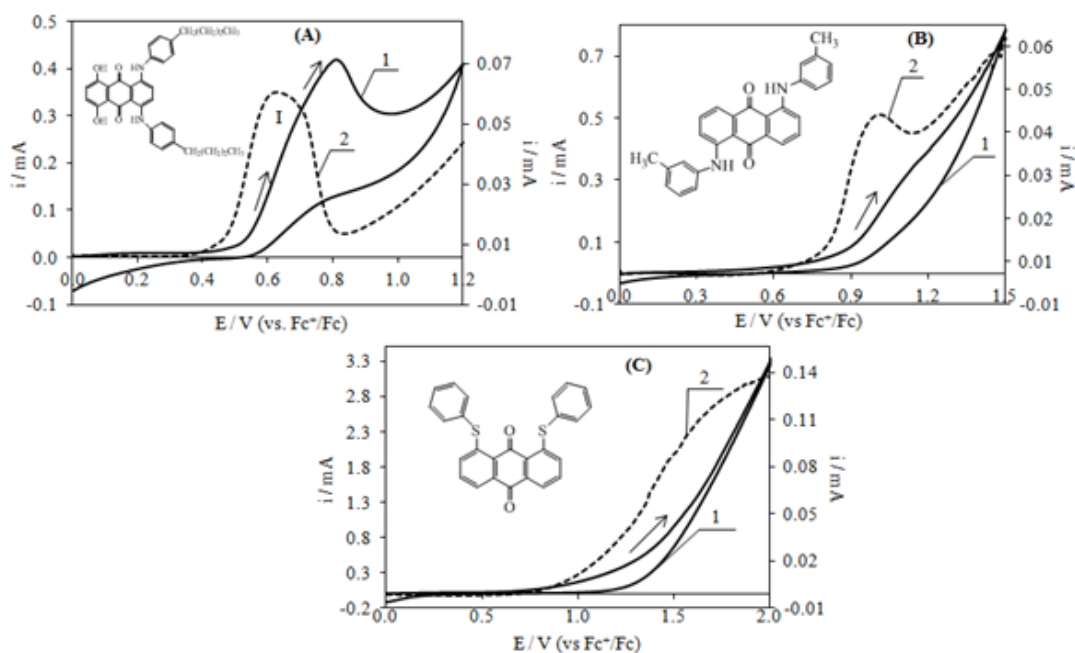


Figure 3. CV (curve 1) and DPV (curve 2) of (A) D3, (B) D4 and (C) D5 oxidation at Pt electrode; $c = 1.0 \times 10^{-3}$ M in 0.1 M $(C_4H_9)_4NClO_4$ in 1-methyl-2-pyrrolidinone; $v = 0.1$ V s^{-1} .

Dyes with low $E_{1/2}$ values tend to react with free radicals. Compounds with lower oxidation potentials have greater ability donate electrons and as a consequence can be considered better antioxidant compounds. On the basis of the values determined for E_{pa} , $E_{pa/2}$, $E_{1/2}$, the anodic transfer coefficient (β_{np}) and heterogeneous rate constant (k_{bh}) were calculated according to the equations presented in previous studies [21, 25] (see Table 2). The heterogeneous rate constant (k_{bh}) determined for a specified potential E characterizes the transfer rate of an electron through the electrode-solution interface. The electron transition coefficient characterizes the symmetry of the activated barrier in an electrode reaction.

Based on the results (Fig. 2 and Fig. 3), it can be concluded that dye D2 showed the greatest tendency for oxidation, as its half-wave potential was the lowest ($E_{1/2} = 0.62$ V). The heterogeneous rate constant (k_{bh}) of this reaction was $2.93 \times 10^{-4} \text{ cm s}^{-1}$. In comparison to D1, D2 and D3 were characterized by lower oxidation potentials, of 0.66 V and 0.72 V, respectively. Of the dyes with $-NH$ R substituents, D4 was the most difficult to oxidize and exhibited the highest values for E_{pa} and $E_{1/2}$ parameters. A very low tendency for oxidation was observed in the case of dye D5, as a weak electrooxidation peak in the voltammograms in the studied potential range. Nevertheless, electron exchanges from the dye to the electrode occurred at the highest rate ($k_{bh} = 4.31 \times 10^{-4} \text{ cm s}^{-1}$). From a thermodynamic point of view, based on the values for $E_{1/2}$ at the first anodic peaks (Table 2), the following qualitative tendency for electron-donation was established: $D5 < D4 < D3 < D1 < D2$.

In this study, the diffusion coefficients (D) of the solvent dyes in non-aqueous media were calculated theoretically using the Hayduk and Laudie equation. The data are present in Table 2 and show that the diffusion ability of the studied dyes was related to their structure [27]. The lowest D were for D1 ($3.44 \times 10^{-6} \text{ cm}^2 \text{ s}^{-1}$), D3 ($3.54 \times 10^{-6} \text{ cm}^2 \text{ s}^{-1}$) and D2 ($3.79 \times 10^{-6} \text{ cm}^2 \text{ s}^{-1}$), which is an indication of their weaker diffusion ability. The common features of these dyes are their branched structures and the presence of aliphatic chains. The molecules of D4 and D5 are less branched in comparison to those of other anthraquinone derivatives and demonstrated the highest diffusion ability, at $4.21 \times 10^{-6} \text{ cm}^2 \text{ s}^{-1}$ and $4.28 \times 10^{-6} \text{ cm}^2 \text{ s}^{-1}$, respectively. High mobility of dye particles in a material can lead to non-uniform color and migration.

Table 2. Values for peak potential (E_{pa}) and half-wave potential ($E_{1/2}$) determined by CV, and anodic transition coefficient ($\beta_{n\beta}$) and heterogeneous rate constant (k_{bh}) determined for $E_{1/2}$ of the first electrode steps in the electrooxidation of dyes at a platinum electrode; $c = 1 \times 10^{-3} \text{ mol L}^{-1}$ in $0.1 \text{ mol L}^{-1} (\text{C}_4\text{H}_9)_4\text{NClO}_4$ in 1-methyl-2-pyrrolidinone, $v = 0.1 \text{ V s}^{-1}$.

Dyes	E_{pa} Istep (V)	$E_{1/2}$ Istep (V)	E_p IIstep (V)	$E_{1/2}$ IIstep (V)	$\beta_{n\beta}$	$D \times 10^6$ ($\text{cm}^2 \text{ s}^{-1}$)	$k_{bh E_{1/2}} \times 10^4$ (cm s^{-1})
D1	0.70	0.66	1.20	1.14	0.52	3.441	2.21
D2	0.65	0.62	1.18	1.07	0.53	3.792	2.93
D3	0.76	0.72	-	-	0.37	3.538	3.03
D4	1.13	1.04	-	-	0.41	4.211	2.67
D5	1.52	1.49	-	-	0.48	4.280	4.31

3.2. Electrochemical reduction of anthraquinone dyes at the Pt electrode

The reduction of dyes in electrode reactions at the platinum electrode were studied by CV and DPV. Figures 4 and 5 show exemplary CV and DPV voltammograms (with higher resolutions) for the dye solutions. The voltammograms presented in Figures 4 and 5 (curves 1 and 2) show that the electroreduction of dyes requires at least two steps at potentials lower than those at which electrolyte decomposition begins. The first step of electroreduction is quasi-reversible, while the second step is irreversible. In the reverse scan, peaks ascribed to the oxidation of dyes in reduced form may be observed.

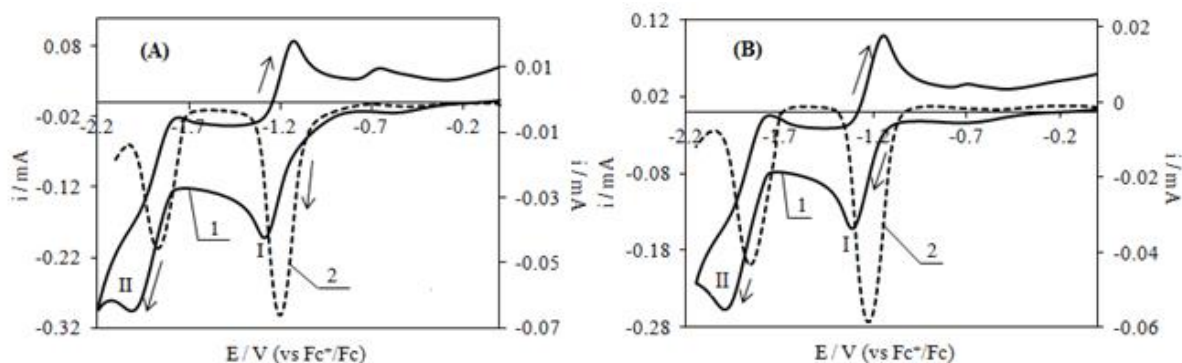


Figure 4. CV (curve 1) and DPV (curve 2) of (A) D1 and (B) D2 reduction at Pt electrode; $c = 1.0 \times 10^{-3}$ M in 0.1 M $(C_4H_9)_4NClO_4$ in 1-methyl-2-pyrrolidinone; $v = 0.1$ V s^{-1} .

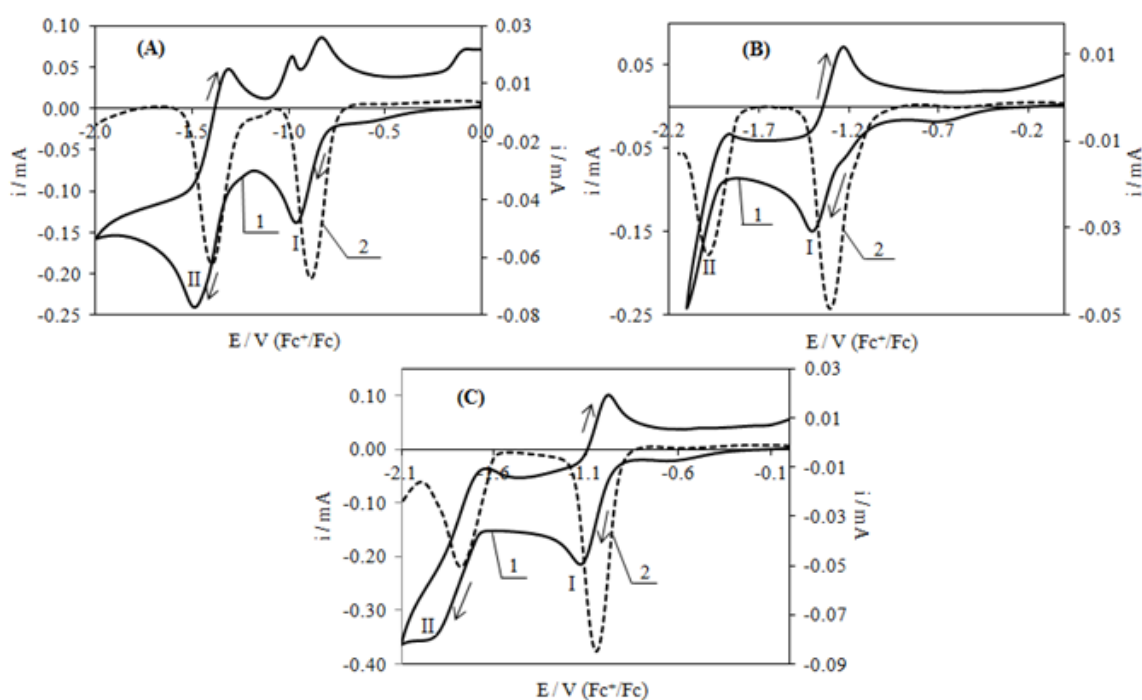


Figure 5. CV (curve 1) and DPV (curve 2) of (A) D3, (B) D4 and (C) D5 reduction at Pt electrode; $c = 1.0 \times 10^{-3}$ M in 0.1 M $(C_4H_9)_4NClO_4$ in 1-methyl-2-pyrrolidinone; $v = 0.1$ V s^{-1} .

As for electrooxidation reactions, the voltammograms (CV and DVP) for the first reduction step under linear diffusion were used to estimate E_{pc} and $E_{1/2}$. Table 3 presents the peak potential results for the investigated compounds.

The $E_{1/2}$ of a peak in the cyclic voltammogram corresponded to the potential of a peak in the corresponding differential pulse curve and was characteristic for each of the subsequent steps in the electrode reductions. The supporting electrolyte $(C_4H_9)_4NClO_4$ in 1-methyl-2-pyrrolidinone did not reveal peaks in the studied potential range and was characterized by only a small capacitive current. The increases in the potentials ($E_{1/2}$) of the anthraquinones were as follows: $D4 < D2 < D1 < D5 < D3$.

Table 3. Values for peak potential (E_{pc}) and half-wave potential ($E_{1/2}$) determined by CV and DPV of the first electrode steps in the electroreduction of dyes at a platinum electrode; $c = 2 \times 10^{-3}$ M in 0.1 M $(C_4H_9)_4NClO_4$ in 1-methyl-2-pyrrolidinone, $\nu = 0.01$ V s $^{-1}$.

Dye	CV				DPV	
	Reduction peaks				Reduction peaks	
	I		II		I	II
	E_{pc} , V	$E_{1/2}$, V	E_{pc} , V	$E_{1/2}$, V	E_{pc} , V	E_{pc} , V
D1	-1.26	-1.21	-2.05	-1.94	-1.19	-1.86
D2	-1.31	-1.27	-1.98	-1.92	-1.23	-1.83
D3	-0.96	-0.92	-1.49	-1.41	-0.89	-1.39
D4	-1.41	-1.37	-1.99	-1.97	-1.31	-1.97
D5	-1.13	-1.08	-1.94	-1.85	-1.04	-1.78

As shown in Table 3, the redox potentials of colorants depend closely on the nature, position and number of the substituting moieties on the anthraquinone molecules. This is related to the formation of hydrogen bonds between the hydroxyl moieties and a neighboring carbonyl group in the dye, which stabilize the resulting radical intermediate, as well as to the varying resonance and inductive effects of groups substituted at different positions in the anthraquinone derivatives [10]. Reduction potentials can be shifted positively or negatively by electron-donating groups. The presence of hydroxyl moieties (in positions 5 and 8) in D3 resulted in a lower shift towards a less negative reduction potential than in the case of D2 and the other anthraquinone chromophore dyes. This behavior can be explained by the resonance or inductive effects of different groups which are substituted at different positions in the considered dyes, as described in other study [28].

3.3. Molecular orbital calculations of dyes using density functional theory

The calculated parameters ($E_{1/2}$ for electrooxidation and $E_{1/2}$ for electroreduction of dyes) were confirmed using quantum chemical calculations. The distribution of the electron charges in the molecules was non-uniform and determined the reactivity of the particular positions (Fig. 6). We observed that chemical bonds located next to a nitrogen atom (in the cases of D1, D2, D3, D4) or a sulfur atom (in the case of D5) were the most susceptible to oxidation.

When an organic material shows a one-electron reversible reduction and oxidation wave, CV is recognized as an important technique for measuring band gaps, electron affinities (LUMO) and potential ionization (HOMO). The oxidation process corresponds to the removal of charge from the HOMO energy level, whereas the reduction cycle corresponds to the addition of electrons to the LUMO. The E_{HOMO} values for all of the studied dyes were determined via calculations and correlation to the $E_{a1/2}$ in the first electrooxidation step, while the E_{LUMO} values were correlated to the $E_{c1/2}$ in the first electroreduction step (Table 4).

The more negative are the values for E_{HOMO} energy, the more difficult it is to oxidize the compound. Lower (more negative) values for E_{LUMO} should correspond to greater (less negative) $E_{c1/2}$ values in electroreduction voltammograms. Despite the fact the colorants had similar structures, a

correlation between E_{LUMO} and $E_{c1/2}$ was not observed. This was most likely related to the different effects of the moieties.

Table 4. Values for half-wave potential $E_{a1/2}$ of electrooxidation, $E_{c1/2}$ of electroreduction, molecular orbital energies E_{HOMO} and E_{LUMO} and the HOMO–LUMO gap (E_{gap}).

Dye	$E_{a1/2}$ (V)	E_{HOMO} (eV)	$E_{c1/2}$ (V)	E_{LUMO} (eV)	E_{gap} (eV)	$E_{a1/2}-E_{c1/2}$ (V)
D1	0.66	-7.894	-1.21	-1.033	-6.861	1.87
D2	0.62	-8.021	-1.27	-1.064	-6.957	1.89
D3	0.72	-7.848	-0.92	-1.132	-6.716	1.64
D4	1.04	-8.379	-1.37	-1.186	-7.193	2.41
D5	1.49	-8.053	-1.08	-1.309	-6.744	2.57

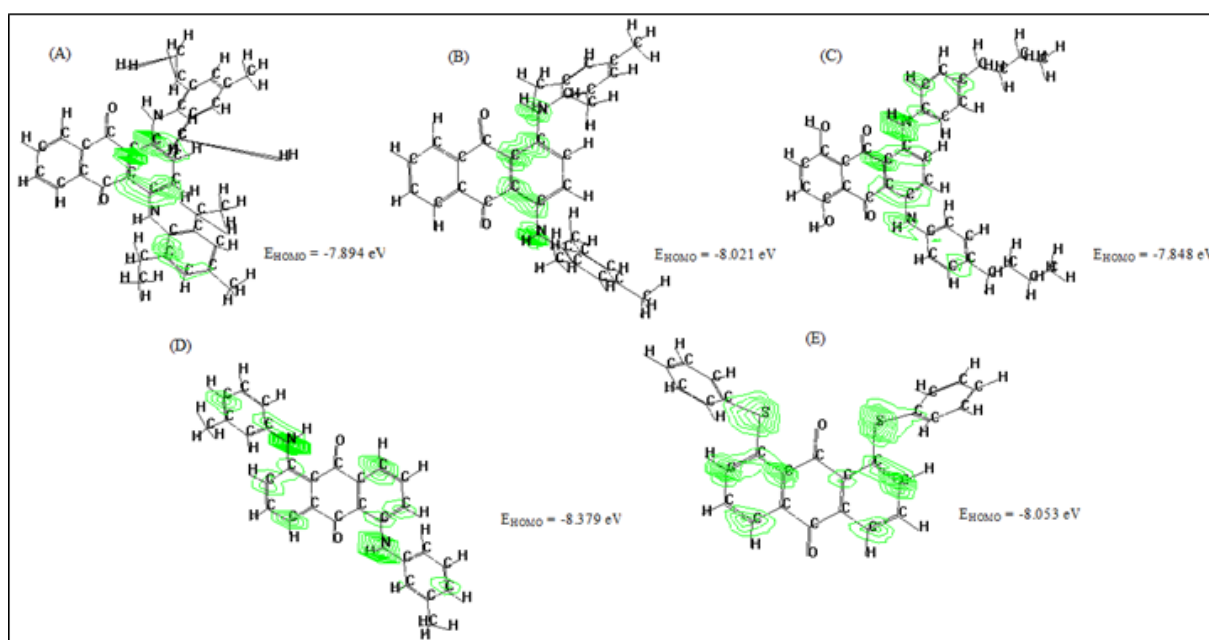


Figure 6. Electron density and probable sites in anthraquinone dyes molecules susceptible to electrooxidation.

The frontier orbital is known to have a strong impact on molecular reactivity. The energy gap, i.e. the energy difference between the HOMO and LUMO, is the quantity of energy which is necessary to change the most stable state of the molecule into an excited state. More positive values for E_{gap} correspond to greater ability to donate electrons and as a result higher antioxidant capacity [18, 29].

$$E_{gap} = E_{HOMO} - E_{LUMO} \quad (7)$$

Based on the values of E_{gap} (Table 2), the following tendency for the antioxidant capacity of the dyes was established: $D4 < D2 < D1 < D3 < D5$. This order presents some differences compared with that based on $E_{1/2}$. These differences may be related to both the geometry and stability of the molecules (energetic properties or dye-related parameters) [30], or with the fact that the E_{HOMO} (which describes

the intrinsic redox activity of the molecules) [31] and E_{LUMO} energies are semi-quantitative parameters for estimating electron affinity, electronegativity and first excitation energy [32]. The highest value for E_{gap} was observed in the case of D5 and the lowest for D4. A linear dependence was found for the theoretically predicted (E_{gab}) and experimentally estimated half-wave reduction potentials of the solvent dyes ($E_{\text{a}1/2}$ - $E_{\text{c}1/2}$). This dependence was not observed in the case of D5, most likely due to the presence of sulfur in the structure. It may be concluded that E_{gap} can be used to correlate the structure of a compound with its ability to transfer electrons.

3.4. Solubility parameters

The solubility of colorants is an important parameter for predicting the miscibility and compatibility of dyes with other materials [33]. The solubility parameters of colorants in EN copolymer were determined using the group contribution method [23]. The solvent dyes were found to exhibit relatively high solubility in the studied EN polymer, imparting in an intense and uniform color at low dye concentrations. The estimated parameters of the dyes together with their components are presented in Table 5.

Table 5. Estimated solubility parameters of studied chromophores.

Name	δ_{d} (MJ/m ³) ^{1/2}	δ_{p} (MJ/m ³) ^{1/2}	δ_{h} (MJ/m ³) ^{1/2}	δ (MJ/m ³) ^{1/2}	$\Delta\delta$ (MJ/m ³) ^{1/2}
D1	20.49	2.46	4.67	21.16	6.05
D2	21.08	2.85	5.03	21.86	7.02
D3	35.04	10.96	8.69	37.73	34.98
D4	22.81	7.09	6.97	24.88	12.51
D5	21.06	4.02	4.56	21.91	7.33

The solubility parameters of dyes depend on the nature of the groups and their location in the molecular structure. Generally, the presence of aliphatic moieties in colorants was correlated with lower values for the investigated parameters. For example, substituting the ethyl groups in D1 colorant ($\Delta\delta = 6.05 \text{ (MJ/m}^3)^{1/2}$) with the ethyl moieties in D2 ($\Delta\delta = 7.02 \text{ (MJ/m}^3)^{1/2}$) resulted in a lower $\Delta\delta$ value, which gave this dye better solubility in the considered copolymer. This observation is in agreement with previously reported data, which revealed that polylactide was more compatible with dyes that contained longer aliphatic moieties [34, 35]. The $\Delta\delta$ value of colorant D3, which has a similar structure to dyes D1 and D2, is significantly higher ($\Delta\delta = 37.73 \text{ (MJ/m}^3)^{1/2}$). This may be because the hydroxyl moieties in D3 increased the number of hydrogen bonding ($\delta_{\text{h}} = 9.96 \text{ (MJ/m}^3)^{1/2}$), thereby decreasing the solubility of this colorant in EN copolymer. These data show that hydrogen bonding has an impact on the solubility properties of the considered compounds.

3.5. Morphology of Dyes

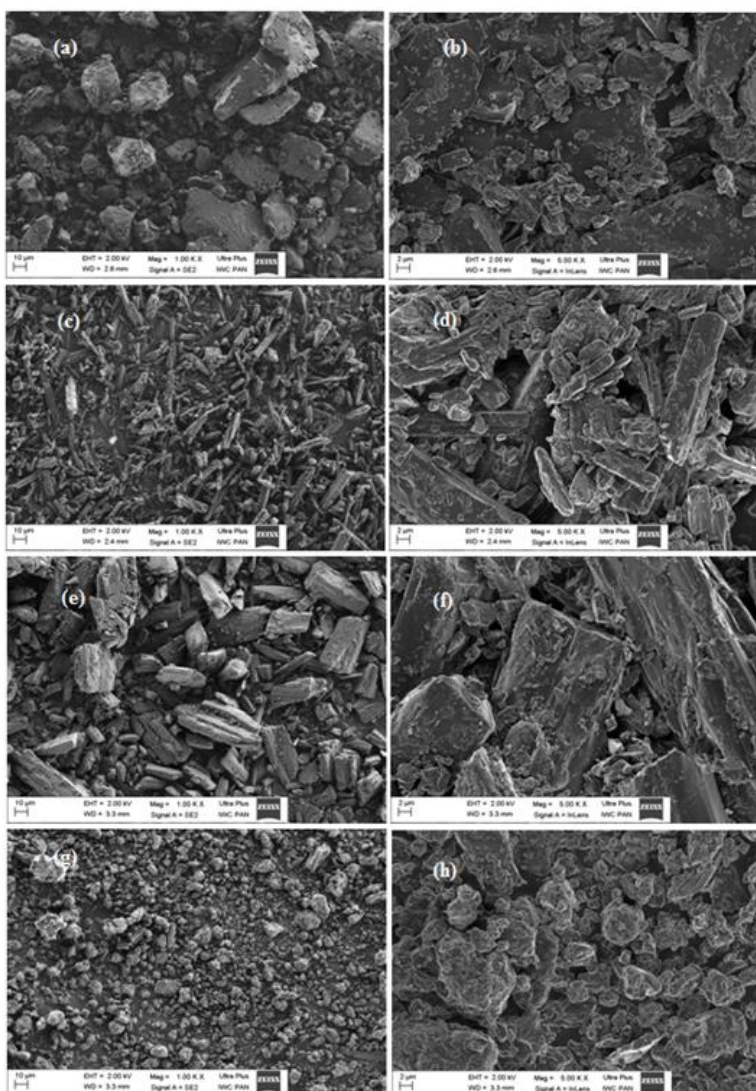


Figure 7. SEM photographs of powder dyes: D1 (a, b), D3 (c, d), D4 (e, f), D5 (g, h).

Scanning electron microscopy (SEM) was applied to study the morphology of the considered dyes. Figure 7 presents SEM photographs of the dye powders at different magnitudes. As can be observed, the crystals of the dyes are different shapes, from rods to plates. Plate structures can be observed for D1 and D5 powders, with particle sizes of approximately 1–20 μm . Needle-like crystals of approximately 5–30 μm in length were observed in dye D3, while D4 showed rod-like crystals.

4. CONCLUSIONS

This study investigated the electrochemical behavior anthraquinone dyes at a Pt electrode. Electroreduction of the studied dyes took place in at least two steps, at potentials lower than the potential at which electrolyte decomposition began. The first step of electroreduction was quasi-reversible, while the second was irreversible. A reverse scan revealed peaks ascribed to oxidation of

dyes in reduced form. From the values for $E_{1/2}$, it was concluded that electron-transfer from the electrode to the dye molecule was easiest in the case of D3 and most difficult for D4. Our results also clearly showed that the oxidation and redox potentials of the anthraquinone molecules were strongly dependent on both the nature and the position of the substituting groups on the dye molecule. Dyes D1 and D2 oxidised in two electrode steps, at potentials below the oxidation potential of the electrolyte. D3 and D4 oxidized in one irreversible step. Only D5, which was characterized by the presence of sulphur, showed a very weak peak in oxidation potentials within the studied range.

From a thermodynamic point of view and based on the values for $E_{1/2}$ at the first anodic peaks, D2 exhibited the greatest tendency for electrooxidation. The structure of D5 lowered its ability to lose electrons and showed the highest oxidative resistance. On the other hand, based on the rate of electron exchange from dye to electrode, the most rapidly oxidized dye was D5, and the most slowly oxidized dye was D1. The first oxidation peak potential (E_{pa} and $E_{1/2}$) values of the studied dyes were evaluated by two electrochemical investigation methods (CV and DPV), enabling a qualitative classification of the compounds depending on the structure and the increase in their electron-donating capacity. These data are consistent with the literature and suggest that voltammetry may provide a useful method for determining the physicochemical properties of such compounds in non-aqueous media.

The HOMO-LUMO gap (E_{gap}) represents a new parameter obtained by computational calculations. E_{ga} can be used as a criterion to correlate the structure of a compound with its ability to transfer electrons. The E_{gap} parameters provided additional information regarding the electron-donating capacity of dyes and showed nonlinear dependence with $E_{1/2}$ values determined by electrochemical measurements.

References

1. D. Keil, R. Flaig, A. Schroeder, H. Hartmann, *Dyes Pigm.*, 50 (2001) 67. DOI: 10.1016/S0143-7208(01)00024-9
2. J. Park, Y. Park, J. Park, *Mol. Cryst. Liquid. Cryst.*, 551 (2011) 116. DOI: 10.1080/15421406.2011.600624
3. M. S. Zakerhamidi, A. Ghanadzadeh, M. Moghadam, *Spectrochim. Acta A*, 79 (2011) 74. DOI: 10.1016/j.saa.2011.02.003
4. M.B. Gholivand, S. Kashanian, H. Peyman, H. Roshanfekar, *Eur. J. Med. Chem.*, 46 (2011) 2630. DOI: 10.1016/j.ejmech.2011.03.034
5. A. Marzec, E. Chrzescijanska, Z. Boruszczak, M. Zaborski, A. Laskowska, G. Boiteux, O. Gain, *Polym. Degrad. Stab.*, 123 (2016) 137. DOI: 10.1016/j.polymdegradstab.2015.11.013
6. E.E. Langdon-Jones, S.J.A. Pope, *Coord. Chem. Rev.*, 269 (2014) 32. DOI: 10.1016/j.ccr.2014.02.003
7. N. Sekar, *Colourage*, 47 (2000) 48.
8. M. Hattori, Kirk-Othmer Encyclopedia of Chemical Technology, John Wiley&Sons Inc. (2005) New Jersey, USA.
9. T. Bechtold, Ch. Fitz-Binder, A. Turcanu, *Dyes Pigm.*, 87 (2010) 194. DOI: 10.1016/j.dyepig.2010.03.026
10. H. Liu, P. Han, Y. Wen, F. Luan, Y. Gao, X. Li, *Dyes Pigm.*, 84 (2010) 148. DOI: 10.1016/j.dyepig.2009.07.013
11. A. Turcanu, Ch. Fitz-Binder, T. Bechtold, *J. Electroanal. Chem.*, 654 (2011) 29. DOI: 10.1016/j.jelechem.2011.01.040

12. R. Shanmugam, P. Barathi, J.-M. Zen, A.S. Kumar, *Electrochim. Acta*, 187 (2016) 34. DOI: 10.1016/j.electacta.2015.11.032
13. E. Chrzescijanska, E. Kusmierk, G. Nawrat, *Polish J. Chem.*, 83 (2009) 115.
14. A. Masek, E. Chrzescijanska, M. Latos, M. Zaborski, *Food Chem.*, 215 (2017) 501. DOI: 10.1016/j.foodchem.2016.07.183
15. A.S. Barham, B.M. Kennedy, V.J. Cunnane, M.A. Daous, *Int. J. Electrochem. Sci.*, 9 (2014) 5389.
16. M. M. Kabanda, I. B. Obot and E. E. Ebenso, *Int. J. Electrochem. Sci.*, 8 (2013) 10839.
17. M. Pordel, S. A. Beyramabadi, A. Mohammadinejad, *Dyes Pigm.*, 102 (2014) 46. DOI: 10.1016/j.dyepig.2013.10.021
18. G. L. Turdean, D. Casoni, C. Sârbu, *J. Iran. Chem. Soc.*, 13 (2016) 945. DOI: 10.1007/s13738-016-0810-5
19. M. Shamsipur, A. Siroueinejad, B. Hemmateenejad, A. Abbaspour, H. Sharghi, K. Alizadeh, S. Arshadi, *J. Electroanal. Chem.*, 600 (2007) 345. DOI: 10.1016/j.jelechem.2006.09.006
20. A. Masek, E. Chrzescijanska, M. Latos, M. Zaborski, *Food Chem.*, 215 (2017) 501. DOI: 10.1016/j.foodchem.2016.07.183
21. Z. Galus, *Fundamentals of electrochemical analysis*, Polish Scientific Publishers PWN (1994) Warsaw, Poland.
22. J. A. Schranke, S. F. Murphy, W. J. Doucette and W. D. Hintze, *Chemosphere*, 38 (1999) 2381. DOI: 10.1016/S0045-6535(98)00433-0
23. D.W. Krevelen, K. Nijenhuis, *Properties of polymers*, Elsevier (2009), Amsterdam, Netherlands.
24. H. W. Milliman, D. Boris, D. A. Schiraldi, *Macromolecules*, 45 (2012) 1931. DOI: 10.1021/ma202685j
25. A. Masek, E. Chrzescijanska, M. Zaborski, *Int. J. Electrochem. Sci.*, 9 (2014) 7904.
26. J. M. P. Q. Delgado, *J. Phase. Equilib. Diff.*, 28 (2007) 427. DOI: 10.1007/s11669-007-9160-4
27. A. Doménech-Carbó, M. T. Doménech-Carbó, M. C. Saurí-Peris, J. V. Gimeno-Adelantado, F. Bosch-Reig, *Anal. Bioanal. Chem.*, 375 (2003) 1169. DOI: 10.1007/s00216-002-1742-8
28. M. Shamsipur, A. Salimi, S. M. Golabi, H. Sharghi, M. F. Mousavi, *J. Solid State Electrochem.*, 5 (2001) 68. DOI: 10.1007/s100089900097
29. I. Ahmad, S. Murtaza, S. Ahmed, *Monatsh Chem.*, 146 (2015) 1631. DOI: 10.1007/s00706-015-1425-8
30. A. Barzegar, M.D. Davari, N. Chaparzadeh, N. Zarghami, J.Z. Pedersen, S. Incerpi, L. Saso, A.A. Moosavi-Movahedi, *J. Iran. Chem. Soc.*, 8 (2011) 973. DOI: 10.1007/BF03246553
31. M.T. Pérez-Prior, R. Gómez-Bombarelli, M.I. González- Sánchez, E. Valero, *J. Hazard. Mat.*, 241-242 (2012) 207. DOI: 10.1016/j.jhazmat.2012.09.028
32. C.-G. Zhan, J.A. Nichols, D.A. Dixon, *J. Phys. Chem. A*, 107 (2003) 4184. DOI: 10.1021/jp0225774
33. R.R. Bommu, T. Nakamura, B.V. Rao, *Colourage*, 47 (2000) 59.
34. D. Karst, Y. Yang, *J. Appl. Polym. Sci.*, 96 (2005) 416.
35. A.F.M. Barton, *Handbook of solubility parameters and other cohesion parameters* CRC Press (1983) Florida, USA.